Preliminary design of the green diesel production process by hydrotreatment of vegetable oils

Javier Moreno Fernández-Villamil[*,1] **and Aurelio Hurtado de Mendoza Paniagua**[*]

[*]Polytechnic University of Madrid (ETSII)

ABSTRACT

In this work, a conceptual design is presented of a HVO/green diesel production unit with a processing capacity of 74 ton/h (500 000 ton/year) of vegetable oils and a production rate of 59 ton/h of diesel. Firstly, an extensive literature review has been conducted regarding the state-of-the-art techniques as well as process equipment, mechanisms of reaction and thermodynamical properties. A market analysis is also presented which estimates feedstock availability and target production rate. With this information, a preliminary Process Flow Diagram is proposed, along with explanations on the type of equipment used and its operating conditions. Process design and simulation has been performed using Aspen Plus®, while Aspen Custom Modeler® has been used to develop more accurate models where necessary. The present study concludes with an analysis of process flexibility, considerations for heat integration and an economic assessment.

KEYWORDS Green diesel; Hydrotreatment of Vegetable Oils; Computer-aided Process Engineering

Introduction

In the last decade, alternative fuels have gained increasing attention from the scientific community, given the growing energy demand and the global warming effect derived from CO_2 emissions. Even though fossil fuels are still the main source of energy across the globe, the European Union has made great effort to change the current situation through the Renewable Energy Directive (RED), which enforces a 20% target for renewable energy sources and a 10% in the transportation sector by the year 2020.

With no more than a year to reach the due date, the EU has been working on a second version of the RED directive, the RED II, which raises the target of renewable energy to 32% by the year 2030 [1]. Given the current paradigm shift, it is clear that changes must be made in the appropriate direction.

The two main biofuels used in transportation are bioethanol used in gasoline and biodiesel or FAME (Fatty Acid Methyl Ester) in diesel. As promising as the word biofuel sounds, there are two main concerns affecting these products which shall be carefully considered. On one hand, engine compatibility makes it undesirable to use blends of more than 7% of FAME in conven-

tional diesel engines, mainly due to its stability and cold flow properties [2]. On the other hand, the sustainability of these processes has been questioned, since the food-based crops that are commonly used as feedstock tamper with food prices and availability in the regions of growth, a problem that has been addressed carefully by Articles 17 and 18 of the RED [3].

In light of the facts, it only seems logical to propose an alternative renewable fuel that is fully compatible with current fossil fuels, as not avoid any changes in the current transportation infrastructure and conventional engines. Green diesel obtained from hydrotreatment of vegetable oils is one, well-established example. Even though it uses the same feedstock as biodiesel, green diesel yields a product with better qualities, which is also indistinguishable from fossil fuel-derived diesel. Table 1 compares the properties of conventional diesel, biodiesel and green diesel.

Hydrotreated vegetable oils (HVOs) seem like a suitable alternative to biodiesel due to their improved cold flow properties, low content in sulfur, aromatics and oxygen, and engine compatibility.

The objective of the present work is to develop a conceptual design for the processing of vegetable oils into green diesel. Technical, economical and environmental aspects will be taken into account as indicators of the quality of the project.

First, a literature review is presented in order to gather the

	Diesel	HVO (NeXBTL)	FAME
CEN standard	EN 590	n/a	EN-14214
Density at 15°C (kg/m^3)	820-845	770-790	860-900
Cetane number	>51	75-99	>51
Higher heating value (MJ/kg)	43.1	44.1	37.2
Blending	<7	0-100	<7
Flash point (°C)	>55	>61	>101
Cloud point (°C)	>-20	>-40	-5

Table 1 Properties of summer diesel, FAME and Neste's green diesel NeXBTL [4].

necessary information for the design of the process and selection between alternatives, followed by a market review to support the financial viability of the venture. The selected process and its variables are then put to test through simulation in Aspen Plus ®, allowing for the optimization of process variables and consumption of utilities through heat integration.

Upon completion of the simulation and technical design stage, an economic assessment will help decide on the economical feasibility of the project and identify main cost contributors. Another, no less important key aspects such as carbon consumption and sustainability of the process are also studied.

Literature review

Literature research for this project attains the technology used for stand-alone processing of vegetable oils into green diesel. Many refiners prefer instead to follow the coprocessing scheme, where vegetable oils are injected into the fuel mixture going to the hydrotreaters in a refinery. Minor investment and revamping is needed with the latter, but the possibility of a 100% renewable fuel is left out. Therefore, this work will focus only in stand-alone processing of HVOs.

Hydrotreatment of vegetable oils could, as a first approach, be compared to the conventional hydrotreatment units used to remove sulfur from refinery products. Annex 1 contains a schematic representation of this process which, when compared with the novel green diesel technologies developed in the last decade, provides substantial proof of the similarity between both hydrotreatment processes.
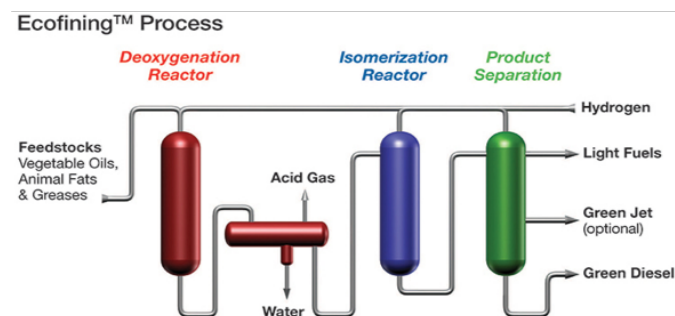

Figure 1 Schematic representation of UOP's Ecofining technology [5].

The two main technologies for hydrotreatment of vegetable oils are NExBTL® by Neste Oil and Ecofining^{TM} by UOP and ENI. The basic scheme for both is quite alike, as can be seen in Figures 1 and 2. Other companies, such as Axens IFP or Haldor Topsoe, have also developed similar technologies by the name of Vegan^{TM} and Hydroflex^{TM}.
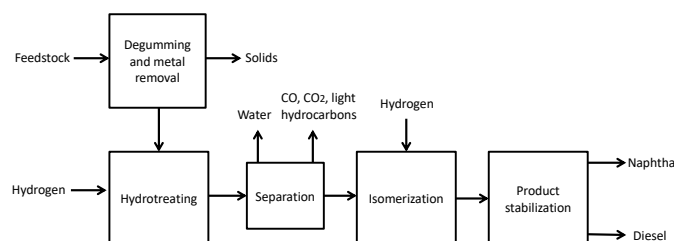

Figure 2 Block diagram for the NExBTL® process [6].

Both processes consist of a primary phase called deoxygenation, where hydrogen is used to break down the triglycerides and eliminate oxygen molecules at high temperatures and pressures. The result is a linear hydrocarbon mixture in the diesel boiling range which is mainly paraffinic, as well as CO, CO_2, water and light hydrocarbons. After separation in a three phase flash tank, the mixture of paraffins is partially isomerized in order to improve its cold flow properties. Isomerization is essential in order to obtain a high quality product, but it comes at the expense of partial loss of the diesel product due to cracking. As a result, a final stabilizer column is needed in order to separate lighter hydrocarbons from the heavier ones, resulting in four possible products: LPG and naphtha as head products, jet fuel and green diesel as bottom product.

Deoxygenation and isomerization take place in presence of catalysts, mainly CoMo and NiMo catalysts for the hydrotreatment section and Pt-based catalysts for the isomerization unit [7]. The conditions in which these reactions take place are what determine the level of cracking, and thus the amount of by-products that are obtained.

Nevertheless, given the need for a flexible and a robust process, the design will include a stabilizing unit which allows to vary the amounts of green naphtha and jet fuel that are obtained, depending on market demand and suitability. Regarding the separation of gaseous products, an amine unit can be used to separate hydrogen, light hydrocarbons, and contaminants such as CO and CO_2.

Feedstock and feedstock pretreament

Before entering the hydrotreating reactor, feedstock must go through a purification unit as to remove any impurities and metals contained in it. Pretreatment becomes indispensable, as it ensures metals (Ca, Mg) and phosphorus will not interfere with the catalysts in the reactor [8].

The pretreatment unit is based on a bleaching unit, and its operating conditions vary depending on the type of feedstock. Bleaching takes place by degumming with addition of an acid such as H_3PO_4, neutralization with NaOH, and washing with demineralized water. In order to further reduce the level of impurities, the feedstock can be fed through silica and/or bleaching earth [9].

There are three feedstock alternatives for this project: palm, rapeseed, and sunflower oil. None of these would allow the final product to enter the second generation biofuels category, but on the other hand they may imply reduced expenses in the pretreatment unit, since they are cleaner than waste oils.

Vegetable oils are made up mostly of triglycerides, which are hydrocarbon structures containing three fatty acid chains and a glycerol backbone in an ester. Processing of these triglycerides will include (I) Saturation of double bonds in the hydrocarbon chains, (II) Separation from the glycerol backbone in the form of propane, and (III) Elimination of oxygen molecules through reduction with hydrogen.
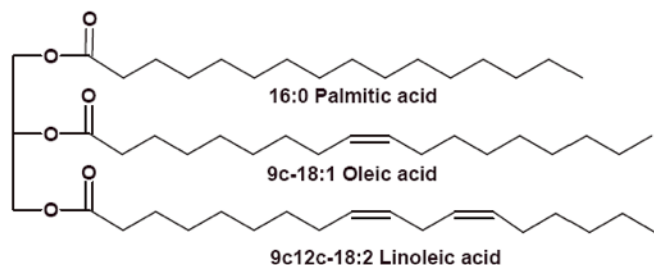

Figure 3 Example of triglyceride structure typically found in palm oil.

One important difference between feedstock types is their iodine value, which refers to the number of double bonds present in the hydrocarbon chains belonging to the fatty acids. A higher iodine number implies a higher number of double bonds and thus an increased consumption of hydrogen when being processed [10]. Table 2 proves that, among the three options, palm oil is the one with a smaller iodine value.

Another important aspect of feedstock is its availability. World production of vegetable oils has increased dramatically in the past decade. As of 2017, world production of vegetable oils and fats is 226 million tons [11]. Top world producers of rapeseed oil include China, Germany, and Canada. Germany produces up to 3.5 million tons of rapeseed oil per year, mainly to feed livestock. Sunflower oil is produced in less quantities, Russia being it biggest producer with an annual average production between 1993 and 2014 of 1.9 million tons.

Palm oil takes the lead in terms of production: 65 million tons per year. This means that palm oil accounts for more than half of the world market share together with soy bean oil. In terms of location, palm oil is mainly grown in tropical countries, Malaysia and Indonesia being its main producers. All production data

Vegetable oil	Iodine value
Canola	110–126
Corn	103–128
Coconut	6–11
Hazelnut	88–90
Olive	77–83
Palm	50–55
Peanut	80–106
Rapeseed	94–120
Sesame	105–107
Soybean	125–130
Sunflower	127–129
Walnut	118–149

Table 2 Iodine value of different vegetable oils [10].

was retrieved from the Food and Agriculture Organization of the United Nations [12].

The final - and probably most important - aspect regarding feedstock selection is price. The surge of interest in biofuels has translated into uncertainty and price volatility in the recent years. Sunflower, rapeseed, and palm oil are all within the category of middle-priced vegetable oils, although palm oil is considerably cheaper than the rest [13]. A better insight of this matter is presented in the Market Analysis section.

Annex 2 contains information on the composition of all three types of feedstock, according to the literature [14-16], as well as practical information about the estimation of their physical properties, according to the fragment approach model proposed by Zong *et al.* [17].

Deoxygenation of vegetable oils

Most of the literature regarding the processing of vegetable oils focuses mainly on its deoxygenation. This is due to the recent interest hydrotreatment processes have sparked in the recent years, but also because companies carefully keep confidential information safe and away from the eyes of the competition.

As a result, there are many questions regarding the mechanism of this process: reaction kinetics, catalyst use and deactivation, and reactor design and conditions. Through this work, the authors have the objective of laying down the basic information regarding this complex process and its simulation.

Basics of deoxygenation of vegetable oils

Many authors have contributed greatly to the understanding of the deoxygenation of VOs [2,18-25]. Out of all of them, the work of Kubicka *et al.* and Tirado *et al.* [26-27] deserve a special mention, due to their outstanding and practical approach on both reaction mechanisms and modeling approaches. While Kubicka has been a prominent researcher in the field, the work of Tirado elaborates a synthesis of previous works regarding reaction kinetics and reactor modeling.

The mechanism of hydrotreatment of triglycerides takes place in two phases. First, double bonds in the hydrocarbon chains are saturated by hydrogen. Then, reduction takes place by the elimination of oxygen atoms through three possible parallel mechanisms: hydrodeoxygenation, decarboxylation and decarbonilation. A schematic representation of this mechanism is shown in Figure 4.

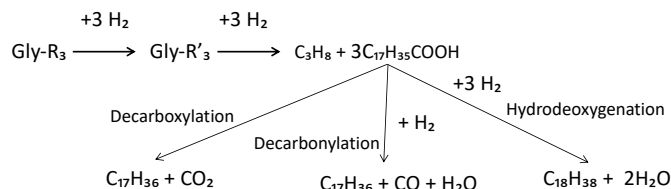As seen in Figure 4, decarbonylation and decarboxylation

Figure 4 Schematic representation of deoxygenation of a typical triglyceride [28].

reactions (DCO) yield paraffins with and odd number of carbons, as fatty acids are usually conformed of an even number of them, whereas hydrodeoxygenation reactions (HDO) yield paraffins with an even number of carbon atoms.

It is unknown whether decarbonylation is part of the process, as the reaction byproduct CO could also be involved in the complex reaction system between CO_2, CO, CH_4 and water that is depicted in Figure 5. As a result, there is no unequivocal evidence to support whether decarbonylation takes place, according to gas chromatograms obtained from different experiments [2, 18-19, 30].
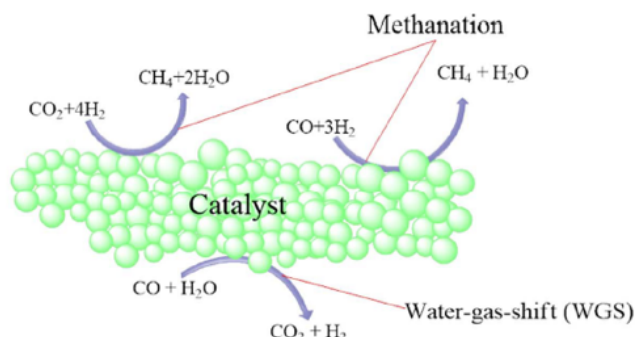

Figure 5 Possible additional reactions taking place alongside deoxygenation [29].

Regarding hydrogen consumption, one could infer from the reaction mechanism depicted in Figure 4 that HDO routes should be avoided, as it consumes three times the amount of hydrogen. However, this would only be true if CO_2 and CO obtained in these reactions didn't take part in the hydrogen-consuming reactions depicted in Figure 5. In fact, if the opposite was to happen, studies confirm as much as 19% more hydrogen would be consumed in the DCO route [2, 26].

Furthermore, the HDO route yields a cleaner green diesel product, as only 3 atoms of carbon per triglyceride are not recovered in the liquid fuel, as opposed to the 6 carbon atoms lost in the DCO route, three more carbon atoms lost in the form of CO and CO_2 which will have to be separated downstream.

Catalyst systems in deoxygenation reactions

Sulphided NiMo and CoMo catalysts supported on alumina are the most common catalysts used in the industrial scale production of green diesel [7]. These are also the same type of catalysts used in conventional hydrotreatment units, which, together with their high activity, explains their widespread use.

The high activity of NiMo /Al_2O_3 catalyst systems allow to reach the 100% conversion rates widely reported in the literature [2, 26, 29]. However, these catalysts need a continuous addition of sulfur-containing agents in order to prevent deactivation, worsening the emission performance of the final product [31].

Nevertheless, given the sulfur-free quality of vegetable oils, green diesel contains less sulfur than conventional diesel [4]. As for the addition of these agents, sulfur concentration in any typical hydrogen feed coming from a conventional hydrotreatment unit in a refinery will suffice.

As alternatives, several studies have focused mainly on the use of sulfur free, noble metals such as Pt and Pd. Whereas NiMo and CoMo sulphided catalysts yield products through both HDO and DCO mechanisms, noble metals show high selectivity for DCO routes, resulting in higher CO2 and CO production [20, 23].

Other disadvantages of noble metals such as Pt or Pd include their high price, lower yields, and rapid deactivation in the presence of sulfur and water. Xin Le *et al.*[29] made a thorough review of these types of catalysts and concluded that, in spite of their cleaner performance, there is still progress to be made in these aspects.

Furthermore, Sotelo-Boyás *et al.*[7] studied the effect of zeolite-supported Pt catalysts and compared them to NiMo/Al_2O_3. He concluded that the stronger acidic sites of the first induced a higher yield of isomerized products at the expense of a higher degree of cracking, with the subsequent loss of valuable diesel product.

As a result, it seems more proper to invest in two separate reactor systems: one for deoxygenation and another one for isomerization. This way, NiMo/Al_2O_3 catalysts can be used to achieve total conversions in the first reactor and, after proper separation of products, cold flow properties can be improved over Pt-zeolites by control isomerization to avoid cracking.

Reactor conditions

When controlling deoxygenation, main reactor variables and conditions are: temperature, pressure, H_2/oil ratio and liquid space hourly velocity (LSHV). As shown in Table 3, typical operating conditions do not vary considerably from one study to another.

In one particular study, Bezergianni *et al.*[32] concluded that increasing reactor temperature above 360 C translated into an undesirable degree of cracking.

In another study, Srifa *et al.*[21] experimented with a wide range of hydrotreating conditions for palm oil over a sulphided NiMo/Al_2O_3 catalyst. Results supported the hypothesis that, under 300°C, partial conversion of triglycerides took place, whereas cracking and isomerization broke down diesel molecules above 360°C.

Regarding H_2/oil ratios, 3 to 5 times the theoretical consumption is recommended in order to ensure gas-to-liquid mass transfer resistance of hydrogen does not play a role of interference in the process [2, 21].

LSHV values, on the other hand, may vary between 1 and 5 h^{-1} [33], although higher values could affect the level of conversion.

Estimation of properties

For the estimation of thermophysical properties in the hydrocarbon mixtures, it is recommended in the literature that the Redlich-Kwong or Peng-Robinson equations of state be used [19,

Study number	Operating conditions	Reference
1	390 C, 50 bar, 1.5 h^{-1}	[34]
2	300 C, 30-50 bar, 1.2 h^{-1}, 500-1500 Nm^3/m^3	[21]
3	300 C, 50 barg, 10-100 h^{-1} (WSHV), 1250 Nm^3/m^3	[2]
4	350 C, 40 bar, 7.6 h^{-1}, 800 Nm^3/m^3	[35]
5	340 C, 40 bar, 1 h^{-1}, 500-1000 Nm^3/m^3	[36]
6	335-360 C, 30-60 bar, 20 mol H$_2$/mol oil	[18]

Table 3 Typical reactor operating conditions for hydrotreatment of vegetable oils over sulphided catalysts, as found in the literature.

27, 37]. If the presence of water is important, then the NRTL property package needs to be included [37]. All of these property packages are included in Aspen Plus®.

Regarding the properties of triglycerides, two methods were found in the literature for their estimation with a reasonable level of precision within less than 10% of error: Zhongs's fragment approach method, which allows to calculate both thermodynamic and transport properties and is illustrated in Annex 2, and Smejkal's group contribution method, which is based in Joback's group contribution method and shows excellent accuracy [17, 38].

Kinetics

Finding proper kinetic data proved to be harder than expected, given the presence of complex triglyceride molecules in the reactions. Furthermore, since the reactions take place in the surface of catalysts, kinetic parameters depend not only in reactor conditions (temperature, mainly) but also in the catalyst system being used.

The team decided that, in order to select appropriate kinetic data among the few options found in the literature, some restrictions had to be put in place:

1. Kinetic data must be calculated in a sulphided NiMo, CoMo catalyst, in order to match catalysts typically used in the industry, as discussed earlier.

2. Reaction pathways for the proposed mechanism must account for the formation of gases typically formed in the HDO and DCO mechanisms that take place in the industrial systems mentioned above (CO, CO$_2$, propane and H$_2$O).

3. Kinetic data must include Arrhenius's constant, so that temperature dependence can be included in the model.

4. If possible, kinetic data should also include the effect of hydrogen pressure in their equations, in order to understand the effect of hydrogen presence in the reactor.

In light of these requirements, the studies of Vélez [18], Landberg [19], Kubicka [26] and Zhang et al.[39] all fit most of them. One of the common and advantageous aspects of all these mechanisms is that they are based on simple power kinetic models, given the incompatibility between more complicated models such as Langmuir-Hinshelwood's and uncertainties linked to operation parameters in trickle-bed reactor systems [40].

As a starting point, Vélez's kinetic studies provide a model which is simple enough to develop a simulation model that converges easily and is exempt of intermediate products. Furthermore, the model is in good agreement with what is known about the mechanism of the hydrotreatment of VOs, as discussed earlier.

Nevertheless, Vélez did not take into account the effect of hydrogen pressure and mass transfer resistance, and the predictions are not accurate enough ($R^2 = 0.8$). Table 4 represents the proposed reaction mechanism.

Once a model that is robust enough is developed, it could be adapted towards another and more sophisticated one, such as that of Kubicka et al. As for Landberg's study, it was discarded as it does not explain the formation of CO$_2$ since it does not take into account the decarboxylation reaction in its proposed reaction pathway.

Hydrogenation of unsaturated triglycerides

$\underset{\text{Trilinolein (LiLiLi)}}{C_{57}H_{98}O_6} + 6H_2 \longrightarrow \underset{\text{Tristearin (SSS)}}{C_{57}H_{110}O_6}$ $r'_1 = k_1 C_{OOO}$

$\underset{\text{Triolein (OOO)}}{C_{57}H_{104}O_6} + 3H_2 \longrightarrow \underset{\text{Tristearin (SSS)}}{C_{57}H_{110}O_6}$ $r'_2 = k_2 C_{LLL}$

Hydrodeoxygenation

$\underset{\text{Tripalmitin (PPP)}}{C_{51}H_{98}O_6} + 12H_2 \longrightarrow \underset{\text{C16:0}}{3C_{16}H_{34}} + C_3H_8 + 6H_2O$ $r'_3 = k_3 C_{PPP}$

$\underset{\text{Tristearin (SSS)}}{C_{57}H_{110}O_6} + 12H_2 \longrightarrow \underset{\text{C18:0}}{3C_{18}H_{38}} + C_3H_8 + 6H_2O$ $r'_4 = k_4 C_{SSS}$

Hydrodecarboxylation

$\underset{\text{Tripalmitin (PPP)}}{C_{51}H_{98}O_6} + 3H_2 \longrightarrow \underset{\text{C15:0}}{3C_{15}H_{32}} + C_3H_8 + 3CO_2$ $r'_5 = k_5 C_{PPP}$

$\underset{\text{Tristearin (SSS)}}{C_{57}H_{110}O_6} + 3H_2 \longrightarrow \underset{\text{C17:0}}{3C_{17}H_{36}} + C_3H_8 + 3CO_2$ $r'_6 = k_6 C_{SSS}$

	k_1	k_2	k_3	k_4	k_5	k_6
$E_a [kJ/kmol]$	149.9	162.5	147.4	149.1	150.6	169.2
$k_0 [1/s]$	9.4×10^{11}	4.4×10^{13}	3.8×10^{10}	5.6×10^{10}	1.4×10^{10}	8.2×10^{11}

Table 4 Proposed mechanism and kinetic data for hydrotreatment of palm oil [18].

Reactor type

Reactors used in this process are most likely the same type of reactors as the ones used in hydrotreating desulphuration units, this is, trickle-bed reactors.

Trickle-bed reactors are excellent choices when it comes to heterogeneous reactions where liquid and gas phases (mainly

hydrogen) come into contact over a catalyst bed at high temperatures and pressures [41].

When compared to other heterogeneous reactors, trickle-beds offer poor heat transfer rates, thus leading to radial temperature gradients and the formation of hotspots. In order to prevent this situation, the reactor may count with interstage quenching systems, cooling jackets or, in more extreme cases, be designed as a multi-tubular reactor. Jeczmionek *et al.*[42] presents a useful study regarding the heat of reactions involved in hydrotreatment of vegetable oils.

Another important aspect of trickle-bed reactor systems are its hydrodynamics. Ranade and Chaudhari [43] present in their book a complete overview of the main parameters affecting the hydrodynamic effects in trickle-bed reactors.

For the estimation of the liquid hold-up in high pressure systems, Larachi *et al.*[44] provides simple correlations based in dimensionless numbers, while the wetting efficiency of the catalyst particles can be estimated with the Reynolds number, according to Giannetto and Specchia [45].

Trickle-bed models were thoroughly reviewed in order to develop a reactor model robust and complex enough to predict with fair accuracy the operation in a hydrotreatment plant for vegetable oils [46-48]. A detailed explanation of the equations used in the model can be found in Annex 4.

Isomerization

Isomerization takes place once gaseous products and water formed during deoxygenation are separated. As discussed earlier, noble metals such as Pt over SAPO zeolite supports are typically used in this operation [29].

Temperatures and pressures are similar to those in deoxygenation, and even if hydrogen is consumed in low quantities, the reaction can only take place in a high pressure hydrogen atmosphere [49].

For simulation, typical conversions found in the literature [50] can be used together with Calemma's proposed pathway and kinetic information for isomerization of long hydrocarbon chains [51].

Market analysis

Figure 6 Oil barrel prices ($/bbl) in the last 4 years [57].

Crude oil prices are the most determining factor for fuel cost. As seen in Figure 6, the price of the barrel has been volatile in the last few months, mainly due to the uncertainty in global economy created by the trade war between China and the U.S. and political problems in Europe [52].

On the other hand, taking a look at the long term outlook of the oil market, supply is ensured due to new deposits being continuously discovered. Regarding the demand for oil and its future prices, experts do not expect the market share to increase, as environmental restrictions in developed countries grow tougher [53].

One such example of these restrictions is the cap for sulfur content in marine fuel, which is being lowered from 3.5 to 0.5% by the International Maritime Organization (IMO) [54]. The measure, which will be effective on the 1st of January of 2020, has brought many discussions to the table as to how to achieve it in the most cost-efficient manner.

As a possible solution, marine vessels could move towards cleaner versions of marine fuel such as low-sulfur diesel blends. In this aspect, green diesel seems like an excellent choice, as its content in sulfur is exceptionally low [4].

The measure, which affects the demand of 3.5 million barrels per day of high-sulfur fuel oil, will likely cause an increase in diesel prices in the future. As of 2018, the mean price of diesel in Spain is 1.1 €/kg [55].

Process capacity and feedstock availability

After studying feedstock prices for vegetable oils (Figure 7), one may notice there is a short gap between retail price for biodiesel and feedstock price. This is also typical for fossil fuel refining products, since the fuels market is close to perfectly competitive.

Figure 7 Biodiesel (FAME) differentials in $/ton [57].

The Finnish company Neste oil, which provides valuable information on the fuel market distribution, proposes a method to fix the price of biodiesel based on margins and production costs which will be used and explained more thoroughly in the Economic Analysis section.

As a result, in order to ensure profitability of the venture, process capacity has to be carefully measured, following the economy of scale principle.

Main players in the HVO game for stand-alone units are, as mentioned earlier, Neste Oil and UOP/ENI. Neste owns 4 production facilities, two in Finland with a capacity of nearly 200,000 tons per year and another two with a capacity of 1000,000 tons per year in Rotterdam and Singapore. As for ENI, they are currently constructing a plant with a capacity of 500,000 tons in Italy [56].

In view of this data, production capacity for the plant is set to be 500,000 tons of green diesel per year, which implies a consumption of around 600,000 tons of vegetable oil per year (roughly 20% is converted into gas and cracking products, according to mass balances).
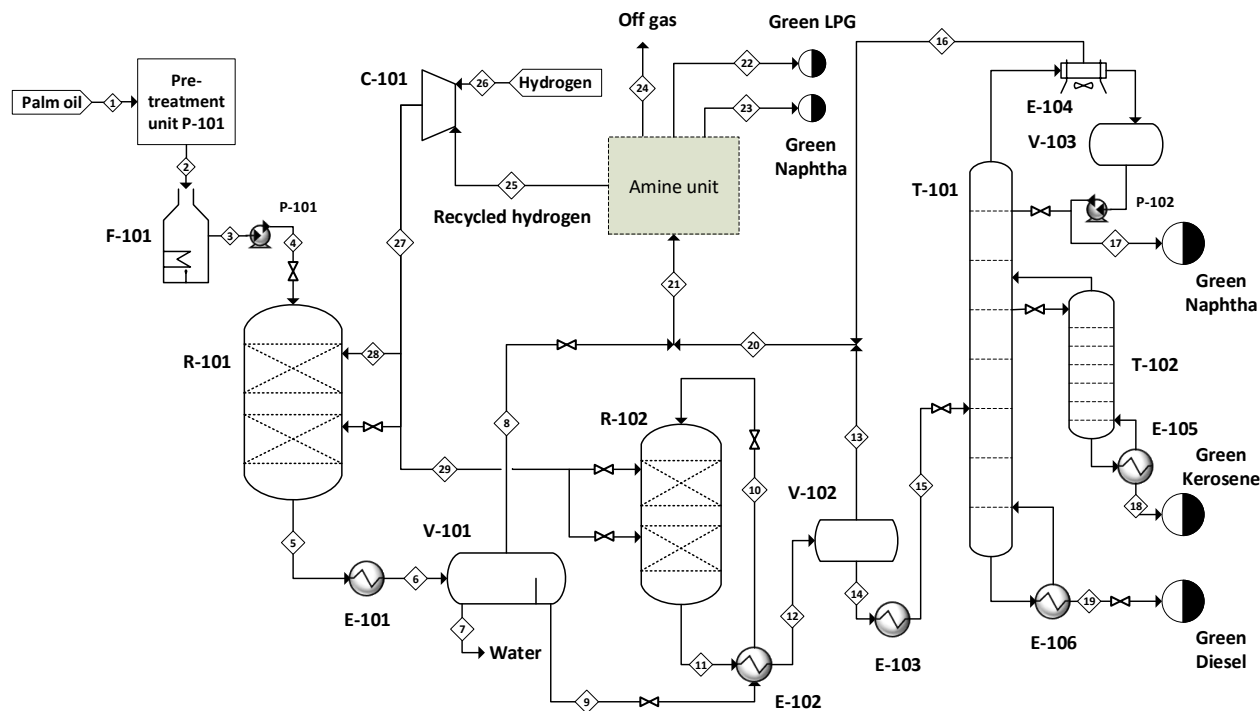
Figure 8 Process flow diagram (PFD) of the proposal for the hydrotreatment of vegetable oils. See corresponding annex for more details on stream characteristics.

As discussed in the Literature Review, only the annual production of palm oil is high enough to ensure feedstock availability.

Furthermore, as seen in Figure 9, palm oil prices are considerably lower than rapeseed and sunflower oil prices, the latter of which is not depicted but data proves its price lands between the two [58].

Figure 9 Vegetable oil prices ($/ton) for rapeseed (above) and palm oil (below) in the last 4 years [57].

The main drivers for choosing palm oil as feedstock in this project are price and availability.

However, the Renewable Energy Directive from the EU demands that GHG emissions be reduced by 60% or more in order to be considered as a biofuel [3].

Oil companies such as Neste and Repsol count with special certifications known as the International Sustainability and Carbon Certifications (ISCC) that ensure biofuel lifecycle from cradle to cradle is sustainable. One representative example depicting control over GHG emissions in the transport of palm oil to the refinery is shown in Annex 3.

Process Design

The information found and portrayed in the Literature Review section allowed the team to perform a conceptual design of the process, the result of which is described in the following paragraphs and depicted in Figure 8. A summary table for the input and output stream conditions is shown in Table 5. A more comprehensive table for all process streams can be found in Annex 6.

The process can be divided into three main sections: hydrotreatment, isomerization, and final product separation. First, palm oil is purified in a pretreatment plant, where it undergoes degumming and bleaching in order to remove metals, phosphorous and any solid particles that might affect the catalyst negatively.

After purification, palm oil enters reactor R-101, which is a trickle bed reactor with catalyst beds disposed in series for intermediate quenching with hydrogen. The catalyst is made of NiMo supported on alumina and conversion is nearly total.

Liquid products obtained in the hydrotreatment reactor are mainly n-alkanes in the diesel boiling range (270-320°C), resulting in a product with high cetane number but poor cold-flow properties. In order to improve the quality of the product, it is essential for the mixture to enter a second reactor.

Reactor R-102 operates similarly to the hydrotreatment reactor, this is, at high temperatures and pressures and with considerable supply of hydrogen gas. In this case, catalyst bed is made of Pt supported in a SAPO zeolite and alumina. Any triglycerides that have not reacted in R-101 will thus finish reacting here.

Improving the cold-flow properties of the product comes at the expense of inevitable cracking of the diesel, which yields

Stream Number	2	26	7	17	18	19	22	23	24
From	(feed)	(feed)	V-101	P-102	E-105	E-106	Amine unit	Amine unit	Amine unit
To	F-101	C-101	(out)	(out)	(out)	(out)	(out)	(out)	(out)
Temperature (ºC)	60	50	30	26	26	26	30	30	30
Pressure (bar)	1,0	20,0	40,0	1,0	1,0	1,0	1,0	1,0	1,0
Enthalpy flow (MW)	-48,92	0,27	-38,70	-0,51	-1,13	-32,71	-3,23	-0,25	-1,76
Mole flow (kmol/h)	87	1296	488	8	11	243	110	5	128
Mass flow (kg/h)	73666	2613	8795	767	1993	58522	4943	377	883
Volume flow (m3/h)	83,50	1760,64	8,82	1,13	2,71	82,58	2741,99	0,60	3201,39
Mass Fractions:									
Tripalmitin	41,97%								
Tristearin	3,75%								
Triolein	46,28%								
Trilinolein	8,00%								
Propane			2,47%				93,47%		
C4H10			2,48%				6,53%		
C5H12			13,91%					84,20%	
C6H14			1,56%					2,28%	
C7H16			26,16%					11,19%	
C8H18			2,25%					0,29%	
C9H20			50,06%					2,05%	
C12H26					4,93%	0,00%			
C13H28					71,67%	0,00%			
C14H30					4,06%	0,04%			
C15H32					1,75%	2,52%			
C16H34					0,27%	9,15%			
C17H36					0,00%	0,65%			
C18H38					0,00%	13,00%			
I-C15					9,73%	2,42%			
I-C16					7,51%	28,89%			
I-C17					0,01%	2,05%			
I-C18					0,06%	41,29%			
Hydrogen		100,00%							25,07%
Carbon dioxyde									64,77%
Water			100,00%	1,10%					10,14%

Table 5 Input (in green) and output (in blue) stream conditions for the proposed Process Flow Diagram.

variable quantities of lower boiling point mixtures such as jet fuel and naphtha, depending on reactor conditions.

The resulting mixtures are separated in a distillation column where naphtha and gaseous products are obtained as top products, diesel as bottom product, and jet fuel is obtained through a side column. This way, the process is flexible enough to yield variable quantities of products different from green diesel, depending on the market demand.

Furthermore, since hydrogen is present in great quantities in both reactors but is not totally consumed, an amine unit was considered as the best option to recover and recycle most of it, as well as the light hydrocarbons and contaminants (CO and CO_2, mainly) present in the gaseous flows which are obtained in the flash tanks situated after each reactor.

The team did not go deeper into the design of the amine unit, as it was assumed the process would be integrated into an existing refinery. However, one interesting option which deserves further investigation would be to study the feasibility of transforming the light hydrocarbons into hydrogen in order to reduce external dependence.

Process simulation and analysis

The proposed solution for the process was simulated using Aspen Plus® V10. Considering that reactor simulation options offered in this software are fairly limited, it was decided that the hydrotreatment reactor would be simulated using its programming modeling environment, known as Aspen Custom Modeler® (see support files).

Explanations for the developed model of the hydrotreatment reactor, which include mass transfer resistance calculations, are explained in detail in Annex 4. From the simulations, it was found that reactor dimensions are 25 meters in length and 5 meters in diameter. Conversion attains 99.9%, at nominal operation pressure (40 bar), slightly varying upon changing the operation conditions.

Regarding the isomerization reactor, only reaction kinetics was modeled using the RPlug block and the proposed reaction pathway and kinetic constants by Calemma et al.[51]. A brief explanation of this model is shown in Annex 5.

Basic calculations were made using typical LSHV values found in the literature for this process [50] and process data. Results provide an estimated reactor size of 18 meters in length

Unit	Process conditions	Comments
P-101	60°C, 1 atm	Below 60°C palm oil is semi-solid
C-101	360°C, 40 bar	Interstage cooling
R-101	300-360°C, 40-60 bar, 10-100 h^{-1} (WSHV), H$_2$/oil ratio 500 Nm^3/m^3	NiMo/Al$_2$O$_3$ catalyst
R-102	360-380°C, 40 bar, 1 h^{-1}, H$_2$/oil ratio 500 Nm^3/m^3	Pt/SAPO-11/Al$_2$O$_3$ catalyst
V-101	30°C, 40 bar	Flash tank
V-102	30°C, 15 bar	Flash tank
T-101	26-300°C, 1 bar	Main column, 28 plates
T-102	215-240°C, 1 bar	Side column, 10 plates

Table 6 Operating conditions for main process equipment.

and 4 meters in diameter, with which a high quality diesel product with excellent cold-flow properties is obtained.

Simulation was useful when testing the fitness of the conditions and data found in the literature, as well as to systematically find and exploit possibilities for process optimization and flexibility (i.e. most important contributors to cost and heat integration options). Such possibilities are analyzed further in this chapter.

Final selected conditions for the main process equipment are shown in Table 6, while the mass and energy balance for all process flows is shown in Annex 6.

Process flexibility

One of the main advantages of simulation is the ability to test the flexibility of the process. This allows to perform a sensitivity analysis and study the effect key design parameters have on the quality and quantity of the product obtained.

Furthermore, evaluating process performance at different operating conditions proves the validity of the models used for simulation. In this case, flexibility of the process was studied for its main operations: hydrotreatment and isomerization.

The use of a custom model for the hydrotreating reactor has allowed for interesting analysis of the influence of operation and feed conditions on overall reactant conversion. Triolein and Tripalmitin being the main reactants in terms of feed composition, the first one is consumed in the first half of the reactor length, while Tripalmitin and Tristearin (generated from hydrogenated Triolein) reactions suffer from competitive inhibition and occur only in the second half of the reactor.

Two variables were found to be critical for reactant conversion: concentration of H$_2$ in the bulk liquid and temperature profile along the reactor.

- Concentration of H$_2$ in the bulk liquid is rather sensitive to pressure variations. A plot of Tripalmitin degree of conversion - the others being higher - against operating pressure can be seen in Figure 10. Note that other operating conditions, such as inlet temperature or cooling power, remain constant for this plot, but can be varied to operate at 40 bar with 99.9% degrees of conversion. A pressure threshold has been observed which varies between 38 and 48 bar, depending on other operating conditions (it is placed at 44 bar
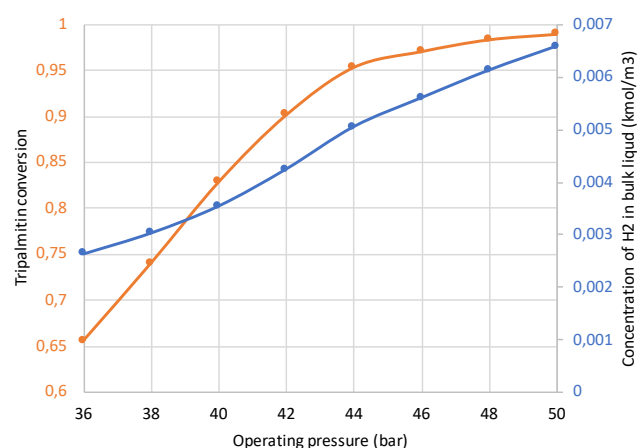

Figure 10 Tripalmitin degree of conversion as a function of operating pressure. In this case, the pressure threshold is placed at 44 bar.

in Figure 10). If pressure becomes lower than this threshold, Tripalmitin conversion will steeply descend, although Triolein conversion is not as significantly affected.

- The temperature profile is also important for reactants' conversion. The fast Triolein consumption in the first half of the reactor causes a great increase in temperature, which must be kept under 360°C with refrigeration. Interestingly, Tripalmitin and Tristearin consumption rates are enhanced by temperatures close to 300°C instead of higher ones. This is due to the higher volatility of hydrogen at higher temperatures, which decreases the amount of H$_2$ in the liquid, and to a worsening of the liquid-solid mass transfer coefficients also at higher temperatures. Temperature profiles should be kept as flat as possible, with higher values for Triolein reactions and lower values for Tripalmitin reaction. Consequently, hydrogen quenching arises as an interesting possibility for refrigeration, something that has nevertheless not been explored in this work.

The reactor performance is not significantly affected by changes in feed composition or feed temperature. In general, it can be said that operation of the hydrogenation reactor is flexible

and that total conversion (> 99.9%) can be achieved in a wide range of situations.

Another interesting study was made regarding isomerization reactor R-102. Operating conditions that affect the degree of isomerization and cracking are: temperature, pressure, LSHV values and H_2/oil ratios.

While the effect of these parameters is studied elsewhere in the literature [50-51, 59-60], the team found most interesting to study the effect of temperature of the reactor. Reactor temperature was varied between 360 and 450°C and the yield of products was evaluated. Of course, this analysis also allowed to understand more deeply which variables had to be manipulated in the distillation columns to adapt to this variation.

As shown in Figure 11, increasing the temperature in R-102 increases the ratio of light to heavy products to the point where at 450°C no diesel is obtained as a product. Another interesting finding was that the proportion of jet fuel is in fact reduced from 420 to 450°C, due to the kinetics of the model.
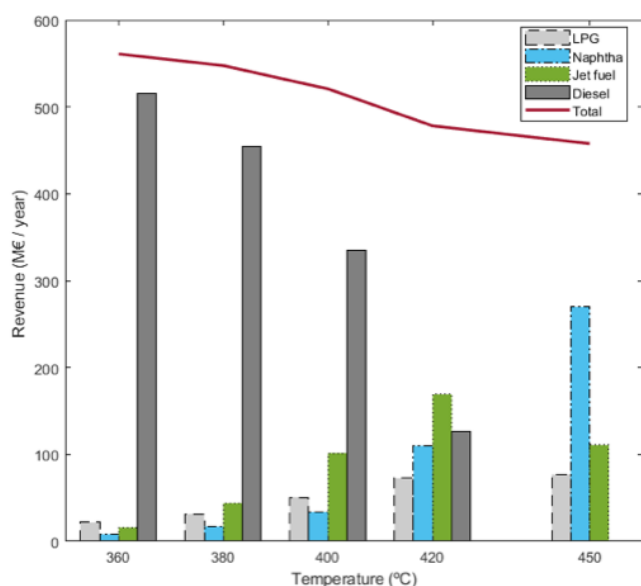

Figure 11 Revenues from LPG, naphtha, jet fuel and diesel obtained at different temperatures in the isomerization (R-102) reactor. Total revenue is shown as a line above.

From this sensitivity analysis it can be concluded that, with current market prices, the process becomes less profitable with increasing temperature of the reactor R-102.

Heat integration

Considerations for heat integration were made according to the pinch analysis results. Aspen Plus®offers an Energy Analysis package that is suitable for this operation.

In order to perform the pinch analysis, only the main process streams were included in the study, all of which flow through a heat exchanger in Figure 8. Thermal fluids for reactor cooling were not considered as options for heat integration.

As for the utilities, cooling water, medium and high pressure steam and fired heat were considered. The composite curve depicting heat flows from the hot and cold currents is depicted in Figure 12.
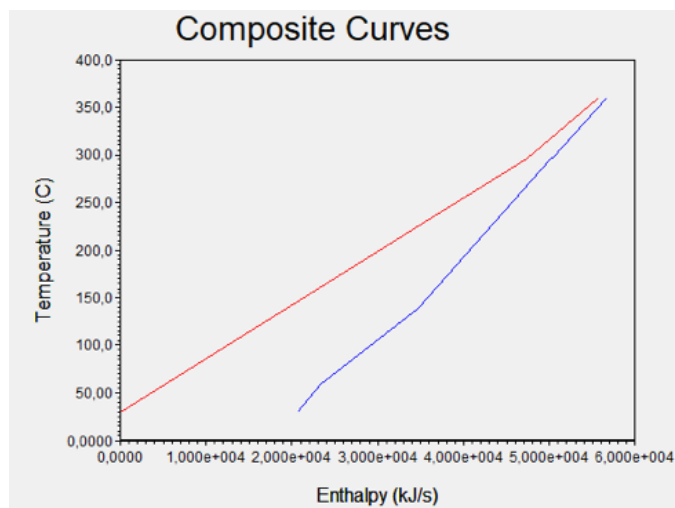

Figure 12 Composite curves for hot and cold flows considered in the pinch analysis. As it can be seen, demand for cold utilities is high given the misbalance between the currents.

The pinch temperature is the highest in the process: 360°C, an interesting result which can be explained by the high power to temperature (kW/°C) ratio of the hot currents coming from the reactors compared to the cold currents. This is a result of the large amounts of hydrogen these hot currents carry.

As a result, the calculated heat exchanger design networks (HEN) do not offer many possibilities, given the misbalance between hot and cold currents and the excess heat being wasted in the process. Table 7 shows the potential savings from the HEN proposal depicted in Figure 13.

Scenario	Base case	Integrated process (unbalanced)	Integrated process (balanced)
Heating (MW)	35,9	1,8	3,7
Cooling (MW)	55,7	145,3	64,1
Operating cost (M€/yr)	3,35	1,12	0,92
Capital cost (M€)	1,84	2,89	3,39
Total cost (M€/yr)	3,6	1,49	1,82
Savings (M€/yr)	-	**2,11**	**1,78**

Table 7 Potential saving from proposed integrated heat exchanger networks over a plant life of 15 years.

To keep a balance, one possibility would be to remove hydrogen in a high temperature flash vessel after each reactor, reducing the power to temperature ratio and thus allowing the pinch temperature to decrease before heat exchange.

The gaseous currents containing mainly hydrogen could then be cooled using air coolers since amine units operate at 30-40°C. Another option would be to design a different unit for hydrogen purification that can operate at higher temperatures, such as a pressure swing absorption unit (PSA).
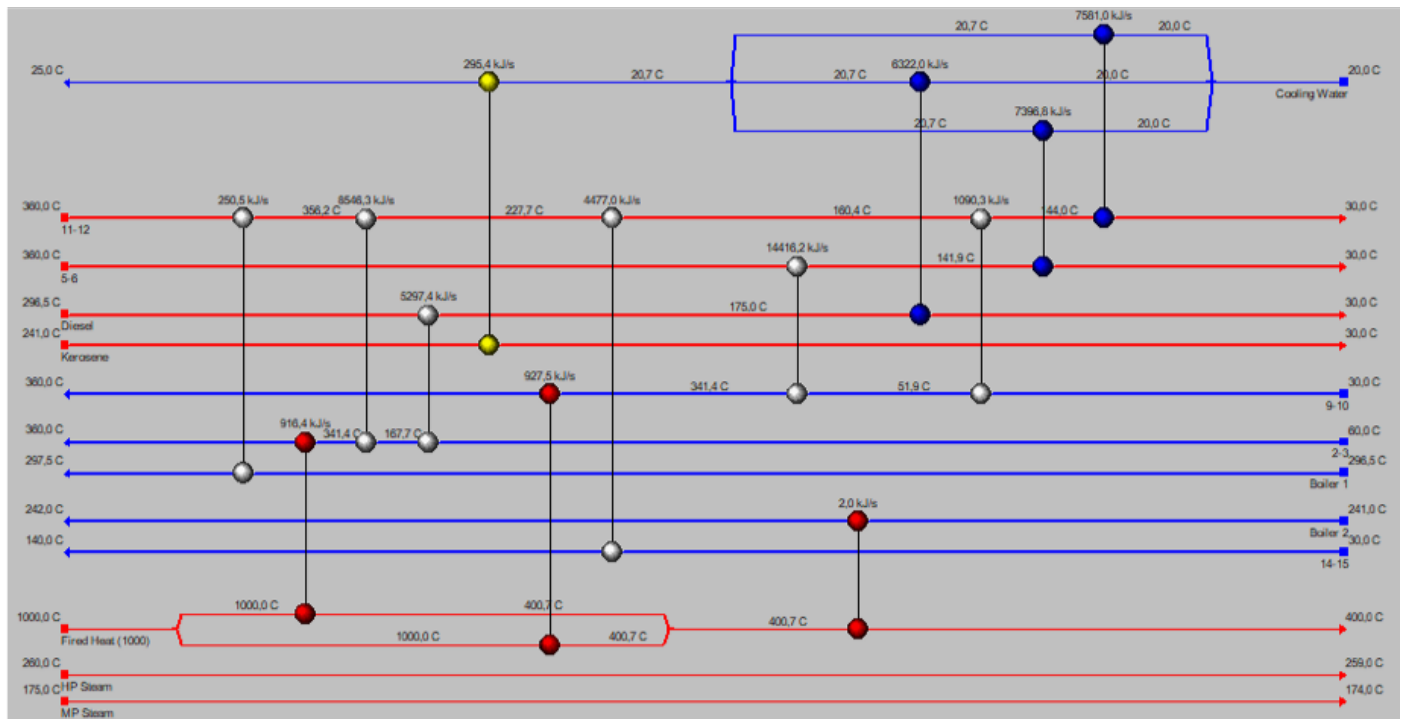
Figure 13 Proposed HEN network for the process. From top to bottom, process flows are: cooling water, stream 11, stream 5, stream 19, stream 18, stream 9, stream 2, boiler from column 1, boiler from column 2, stream 14, fired heat, high pressure steam and medium pressure steam. Minimum temperature difference is $10°C$ ($9{,}7°C$ in yellow exchanger)

Propane reforming

From stream 22 in the Process Flow Diagram (8) it can be seen propane could be utilized for hydrogen generation through steam reforming:

$$C_3H_8 + 6\,H_2O \longrightarrow 3\,CO_2 + 10\,H_2 \tag{1}$$
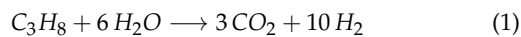
Since 105 kmol per hour of propane are obtained and the required input for hydrogen is 1296 kmol per hour, propane could cover 80% of the hydrogen consumption, while the rest could be obtained from methane reforming, thus reducing its negative greenhouse impact.

Economic analysis

The economic evaluation of the project starts by calculating the capital cost of the plant and the variable production costs using Towler and Sinnot's method [61]. Product price is then calculated according to the margin method proposed by Neste oil, where margins are applied in order to obtain a reasonable benefit.

Payback period and net present value are also calculated, and sensitivity analysis is performed in order to check the dependence of project profitability on the main contributors to cost.

Capital investment

Sizes and capacities for the main process equipment are obtained through simulation. Costs are then calculated using curves for each process equipment from Turton [62] and Rules of Thumb in Engineering Practice [63], while the cost for the heat exchanger network was already obtained in the heat integration section. Costs must be updated using CEPCI index for 2016, which is 541,7.

ISBL costs are calculated as the sum of equipment costs multiplied by Lang installation factors, while OSBL, engineering and contingency costs are calculated as percentages of the inside battery limits cost (30, 30 and 10%, respectively).

Finally, working capital is estimated as 15% of the fixed capital investment in order to obtain the total required investment. Tables 8 and 9 sum up these results.

Equipment	Cost (M€)
Reactor R-101	91,3
Vessel V-101	0,2
Reactor R-102	39,8
Vessel V-102	0,3
Tower T-101	0,2
Tower T-102	0,04
Compressor C-101	9,4
Heat exchangers	10,8
Pretreatment unit	10
Total	**162,0**

Table 8 Main process equipment costs (installed).

As expected, biggest contributors to capital investment are reactor costs. As much as 29% of the total investment is coming from the hydrotreatment reactor, a value which gives perspective on the importance of its design.

Investment of the plant seems to be in line with the €550 million which Neste Oil is estimated to have invested in its plant

Investment	Cost (M€)
ISBL	162,0
OSBL	48,6
Engineering	48,6
Contingency	16,2
Fixed cap. Inv.	275,4
Working cap.	41,3
Total investment	**316,7**

Table 9 Total capital investment of the venture.

Production costs

Variable costs come from raw materials, utilities consumption, fungibles (catalysts) as well as waste stream treatment. Reference costs for utilities and waste water treatment were taken from Aspen Plus® and Turton except for the price of electricity, which was fixed at 83 €/MWh, according to the values for industrial consumption in Spain [65].

Cooling duty for the reactors was calculated using Aspen Plus®, according to the heat of reactions. It is assumed that part of this heat is absorbed by the hydrogen gas (quenching), although half of it is estimated to be removed by a thermal fluid, which also needs to be considered.

The price of hydrogen purification in an amine unit was estimated as 0,1€ per treated m^3, three times its typical value in order to account for handling expenses [66].

Catalyst prices were estimated based on their Ni, Mo and Pt content as found in the literature and their price [21, 50]. Lifecycle of the catalyst was assumed as 1,5 years, based on typical hydrodesulfuration catalyst lifecycles [67].

Regarding feedstock, palm oil price is selected as 0,7 €/kg a base case scenario, based on the recent values shown in the Market Analysis. Hydrogen price, on the other hand, is fixed at 1 €/kg, assuming it can be generated within the plant.

Fixed costs are calculated assuming the plant is two operators are present at all times and a base salary of €50,000 per year. The rest of the costs can be calculated as percentages of labor and investment (ISBL and OSBL) costs, including: supervision, maintenance, property taxes, plant overhead, royalty fees and depreciation. For the latter, 5% of fixed capital cost was considered, assuming a plant life of 20 years.

Calculations for all costs as well as estimation details can be found in Annex 7. The proportion of production costs is depicted in Figure 14. The results confirm what was found in another similar study [68], where the cost of the raw material accounted for 75% of the production costs.

Given the volatility of the price for palm oil and its weight on the production costs, it is highly recommended in view of these results that future studies in the field focus on the possibility of adapting the process to less clean (but cheaper) waste oils such as cooking oil or oil from the fish and animal industry.

Product price and profitability

Product price and revenue can be calculated by adding margins to production costs and comparing the result with current
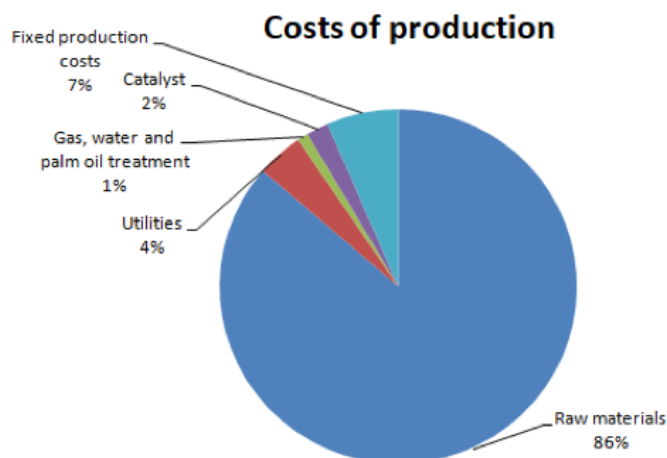

Figure 14 Operating costs of the plant.

Raw materials	Consumption (t/yr)	Cost (€/kg)	Cost (M€/yr)
Hydrogen	20901,5	1	20,9
Palm oil	589331	0,7	412,5
Utilities	**Consumption (MW)**	**Cost (€/MWh)**	**Cost (M€/yr)**
Cooling	145,3	0,08	0,089
Heating	1,8	1,5	0,023
Electricity	31,4	83	20,85
Thermal fluid	11,9	2	0,19
Gas, water and palm oil treatment	**Flow (Mm3/yr)**	**Cost (€/m3)**	**Cost (M€/yr)**
Water	0,7	0,043	0,03
Hydrogen purification	44,9	0,1	4,49
Palm oil purification	0,7	0,5	0,37
Fungibles	**Consumption (t/yr)**	**Cost (€/kg)**	**Cost (M€/yr)**
NiMo/Al2O3	81430,3	4,2	0,65
Pt/SAPO-11	72382,464	139,5	10,10
Total variable costs			**470,2**

Table 10 Summary review of the variable cost of production.

market values for biodiesel to ensure competitiveness of the product.

Plant production is roughly 468.000 metric tons per year of green diesel. Byproducts include: green jet fuel (15.900 t/yr), green naphtha (9.100 t/yr) and green LPG (39.500 t/yr).

Table 11 shows the calculated margin for green diesel produced in the process, considering a market value of 1,1 €/kg. The rest of the product prices are: 1€/kg for kerosene, 1,15 €/kg for naphtha, and 0,54 €/kg for LPG, according to the Spanish market [55]. The values obtained in Table 9 are similar to those shown by Neste Oil for their Renewable product margin estimation, although final margin values for Neste Oil are twice as high [69], probably due to tax exemptions and the high quality of the diesel which allows it to be sold at higher prices.

To calculate profitability of the plant, annual cash flow is determined considering the EBIT value obtained after subtracting production costs to revenues and a taxation of 15% over profits,
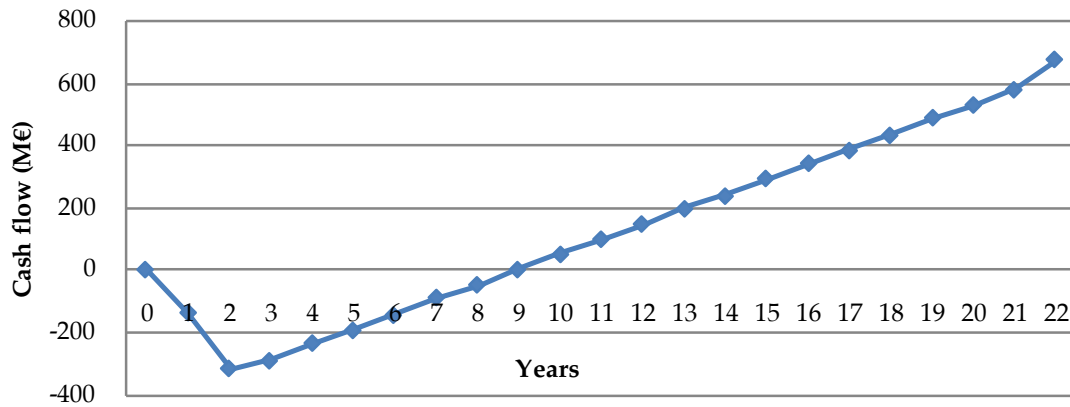
Figure 15 Cash flow over the lifespan of the plant and its construction, in M€.

	Green Diesel
Production (t/yr)	468175
Cost of palm oil (€/t)	700
Variable cost of production (€/t)	121,8
Fixed cost of prod (€/t)	70,1
Margin (€/t)	**208,1**
Final product cost (€/t)	**1100**

Table 11 Product margin for a market value of green diesel of 1,1 €/kg.

due to the environmental value of the project.

Depreciation was considered as a linear function over the plant's lifespan of 20 years (5%), as shown in the fixed costs of production. A realistic approach was used where the plant undergoes technical shutdowns once every two years, reducing its productivity to 90%. Furthermore, productivity on the first year was assumed to be 75% due to technical difficulties in start-up operations.

Annual cash flow is shown in Figure 15, where it can be noticed that the slope of the curve varies every two years due to the above-mentioned scheduled technical shutdowns. Also, construction of the plant is 2 years.

As seen in Figure 15 (for which the values are shown in Annex 7), payback period is 7 years. In order to determine the economic interest of the project, net present value has been used. The net present value or NPV can be calculated from the cash flow in each year and the discount rate, which is around 10%. However, since the interest rate depends on several factors and is hard to predict at this stage, the net present value has been calculated at different interest rates varying from 6 to 14%.

As seen in Figure 16, negative NPV values are not positive except for low values, a consequence of the high investment cost the project requires.

Considering palm oil and diesel prices are of decisive importance for the profitability of the venture, a sensitivity analysis was performed to study the effect of their fluctuation on the feasibility of this project. Palm oil prices are varied between 900 and 500 €/ton, while diesel prices are varied between 0,9 and 1,3 €/kg.

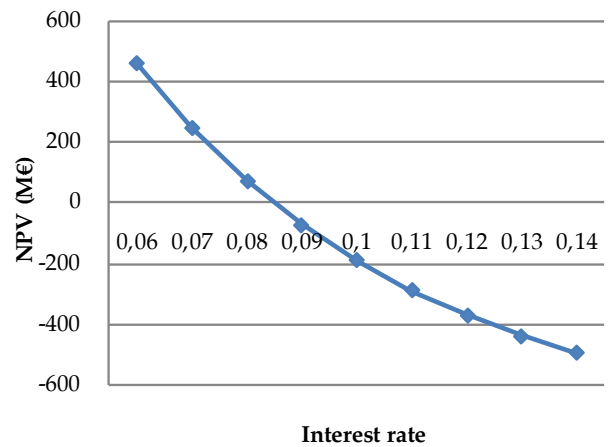Table 12 represents the payback period and NPV for both

Figure 16 Net Present Values at interest rates from 6% to 14%.

analyses. As seen from the results, these variations have great effect over the results, both in a positive and in a negative way.

Diesel price (€/kg)	Payback period (yr)	NPV (M€)
0,9	Negative cash flow	-
1,3	3	4149
Palm oil price (€/t)	**Payback period (yr)**	**NPV (M€)**
500	3	5330
900	Negative cash flow	-

Table 12 Sensitivity analysis results on profitability for diesel and palm oil prices.

Conclusions

The EU's Renewable Energy Directive RED is imposing ambitious improvements in the energy market in order to shift Europe's energy mix towards a more sustainable selection of fuels.

In this regard, biofuels from vegetable oils are a valid option to allow the transition in the energy market, although regulations and process design should consider the sustainability of

the feedstock very closely for both plantation and transport.

Furthermore, the high effect feedstock price has over process profitability should invite designers to consider alternative sources of oils such as waste products from the fish and animal industries or used cooking oil.

When hydrotreated and isomerized, vegetable oils not only yield a cleaner, high quality product, but also present improved cold flow properties, making it an attractive product in northern European countries.

In this design, a plant with a capacity of roughly 500,000 tons per year of green fuel (diesel, kerosene, naphtha and LPG) has been proposed, simulated, and its feasibility evaluated.

The team found that, main aspects considered, the design of the hydrotreatment reactor is essential to ensure total conversions and profitability. This importance is corresponded with proper design through simulation in Aspen Custom Modeler®.

Moreover, the isomerization reactor allows shifting the production in the desired direction, allowing to adapt the process to market demand.

Regarding heat integration, the team found an imbalance between cold and hot streams in the process, making heat integration difficult and resulting in an excess of heat for which future investigations are needed. Another possible process improvement includes propane steam reforming to obtain hydrogen, as calculations show that it could cover 80% of its consumption rate.

Finally, the economic analysis shows a profitable process after the 7th year, although diesel and palm oil fluctuations make it a risky investment. In order to improve this situation, funding and governmental incentives would be needed.

Acknowledgements

References

[1] Proposal for a Directive of the European Parliament and of the Council on the promotion of the use of energy from renewable sources. Corrigendum from the COM(2016) 767 document, made at Brussels in 23/02/2017.

[2] Rasmus G. Egeberg, Niels H. Michaelsen, Lars Skyum. Novel hydrotreating technology for production of green diesel. Haldor Topsoe.

[3] Official Journal of the European Union. Directive 2015/1513 of the European Parliament and of the Council of 9 September 2015 amending Directive 98/70/EC relating to the quality of petrol and diesel fuels and amending Directive 2009/28/EC on the promotion of the use of energy from renewable sources. Art. 17 and 18.

[4] Neste Renewable Diesel Handbook. Neste Corporation, May 2016.

[5] UOP, 2012. UOP/ENI Ecofining™ Process. www.uop.com

[6] Nils-Olof Nylund, Kimmo Erkkila, Matti Ahtiainen. Optimized usage of NExBTL renewable diesel fuel. VTT, 2011.

[7] Rogelio Sotelo-Boyás, YangYong Liu, Tamoaki Minowa. Renewable Diesel Production from the Hydrotreating of Rapeseed Oil with Pt/Zeolite and NiMo/Al2O3 Catalysts. I&EC Research. Ind. Eng. Chem. Res. 50 (2011), pp. 2791-2799.

[8] W. Kiatkittipong, S. Phimsen, K. Kiatkittipong, S.Wongsakulphasatch, N. Laosiripojana, and S. Assabumrungrat. Diesel like hydrocarbon production from hydroprocessing of

[9] Neste Oil, 2012. NExBTL® Renewable Diesel Singapore Plant. Tallow pathway description.

[10] María Cecilia Vásquez, Electo Eduardo Silva, Edgar Fernando Castillo. Hydrotreatment of vegetable oils: A review of the technologies and its developments for jet biofuel production. Biomass and Bioenergy 105 (2017) pp. 197-206.

[11] Food and Agriculture Organization of the United Nations. Food Outlook, July 2018.

[12] FAO, www.fao.org, faostat/crops processed. Information retrieved in December 2018.

[13] R.E.A. Holdings PLC. www.rea.co.uk/markets. Information retrieved in December 2018.

[14] Graboski MS, McCormick RL. Prog Energ Combust 24 (1998), pp. 125-64.

[15] Pryde EH. Northern Regional Research Center, US Department of Agriculture, Peoria, Illinois, The American Oil Chemists' Society, Champaign, IL (1979).

[16] M. Snare, I. Kubickova, P. Maki-Arvela, D. Chichova, K. Eranen, D.Yu. Murzin. Catalytic deoxygenation of unsaturated renewable feedstocks for production of diesel fuel hydrocarbons. Fuel 87 (2008), pp. 933-945.

[17] Li Zong, Sundaram Ramanathan, and Chau-Chyun Chen. Predicting Thermophysical Properties of Mono- and Diglycerides with the Chemical Constituent Fragment Approach. Ind. Eng. Chem. Res. 49 (2010), pp. 5479-5484.

[18] Juan Felipe Vélez Manco. Conceptual Design of a Palm Oil Hydrotreatment Reactor for Commercial Diesel Production. Master's thesis within the chemical engineering program at Universidad Nacional de Colombia, 2014.

[19] Katarina Landberg. Experimental and Kinetic Modelling Study of Hydrodeoxygenation of Tall Oil to Renewable Fuel. Master's thesis within the Innovative and Sustainable Engineering program. Chalmer's University of Technology. Gothenburg, Sweden, 2017.

[20] M. Snare, I. Kubickova, P. Maki-Arvela, K. Eranen, J. Warna, D.Yu. Murzin. Production of diesel fuel from renewable feeds: Kinetics of ethyl stearate decarboxylation. Chemical Engineering Journal 134 (2007), pp. 29-34.

[21] Atthapon Srifa , Kajornsak Faungnawakij, Vorranutch Itthibenchapong, Nawin Viriya-empikul, Tawatchai Charinpanitkul, Suttichai Assabumrungrat. Production of bio-hydrogenated diesel by catalytic hydrotreating of palm oil over NiMoS$_2$/γ-Al$_2$O$_3$ catalyst. Bioresource Technology 158 (2014), pp. 81-90.

[22] Worapon Kiatkittipong, Songphon Phimsen, Kunlanan Kiatkittipong, Suwimol Wongsakulphasatch, Navadol Laosiripojana, Suttichai Assabumrungrat. Diesel-like hydrocarbon production from hydroprocessing of relevant refining palm oil. Fuel Processing Technology 116 (2013), pp. 16-26.

[23] R. W. Gosselink, S. A. W. Hollak, S.-W. Chang, J. van Haveren, K. P. de Jong, J. H. Bitter, D. S. van Es. Reaction Pathways for the Deoxygenation of Vegetable Oils and Related Model Compounds. ChemSusChem Reviews, pp. 1-20.

[24] Pavel Simácek, David Kubicka, Gustav Sebor , Milan Pospísil. Hydroprocessed rapeseed oil as a source of hydrocarbon-based biodiesel. Fuel 88 (2009), pp. 456-460.

[25] Pavel Simácek, David Kubicka, Iva Kubicková, Frantisek Homola, Milan Pospísil, Josef Chudoba. Premium quality renewable diesel fuel by hydroprocessing of sunflower oil. Fuel 90 (2011), pp. 2473-2479.

[26] David Kubicka, Vratislav Tukac. Chapter Three - Hydrotreating of Triglyceride-Based Feedstocks in Refineries. Advances in Chemical Engineering 42 (2013) , pp. 141-194.

[27] Alexis Tirado, Jorge Ancheyta, and Fernando Trejo. Kinetic and Reactor Modeling of Catalytic Hydrotreatment of Vegetable Oils. Energy Fuels 32 (2018), pp. 7245-7261.

[28] I. Karame, in Hydrogenation, 1st ed. (Eds: R. Sotelo-Boyas, F. Trejo-Zarraga, F. J. Hernandez-Loyo), InTech, Winchester, UK 2012, Ch. 8.

[29] Xin Li, Xingyi Luo, Yangbin Jin, Jinyan Li, Hongdan Zhang, Aiping Zhang, Jun Xie. Heterogeneous sulfur-free hydrodeoxygenation catalysts for selectively upgrading the renewable bio-oils to second generation biofuels. Renewable and Sustainable Energy Reviews (2017).

[30] Juan Tapia, Nancy Y. Acelas, Diana López and Andrés Moreno. NiMo-sulfide supported on activated carbon to produce renewable diesel. Universitas Scientiarum, 22 (2017), pp. 71-85.

[31] Hachemi I, Jenistova K, Maki-Arvela P, Kumar N. Comparative study of sulfur-free nickel and palladium catalysts in hydrodeoxygenation of different fatty acid feedstocks for production of biofuels. Catal. Sci. Technology 6 (2016), pp. 1476-87.

[32] Stella Bezergianni, Aggeliki Kalogianni. Hydrocracking of used cooking oil for biofuels production. Bioresource Technology 100 (2009), pp. 3927-3932.

[33] Graca I, Lopes JM, Cerqueira HS, Ribeiro MF. Bio-oils upgrading for second generation biofuels. Ind. Eng. Chem. Res. 52 (2012), pp. 275-87.

[34] Luca Zullo - VerdeNero LLC. Green Jet and Green Diesel Second Generation Biofuel. Powerpoint presentation available at https://www.auri.org/assets/2013/05/Auri-April-30-2013-zullo.pdf. Last consulted on the 25th of December of 2018.

[35] Yanyong Liu, Rogelio Sotelo-Boas, Kazuhisa Murata, Tomoaki Minowa, and Kinya Sakanishi. Hydrotreatment of Vegetable Oils to Produce Bio-Hydrogenated Diesel and Liquefied Petroleum Gas Fuel over Catalysts Containing Sulfided Ni-Mo and Solid Acids. Energy Fuels 25 (2011), pp. 4675-4685.

[36] Mikulec J, Cvengros J, Joríková L, Banic M, Kleinová A. Second generation diesel fuel from renewable sources. J Cleaner Prod 18 (2010), pp. 917-26.

[37] Carlo Edgar Torres-Ortega, Jian Gongb, Fengqi Youb, Ben-Guang Ronga. Optimal synthesis of integrated process for coproduction of biodiesel and hydrotreated vegetable oil (HVO) diesel from hybrid oil feedstocks. Proceedings of the 27th European Symposium on Computer Aided Process Engineering - ESCAPE 27. October 2017. Barcelona, Spain.

[38] Quido Smejkala, Lenka Smejkalová, David Kubick. Thermodynamic balance in reaction system of total vegetable oil hydrogenation. Chem. Eng. Journal 146 (2009), pp. 155-160.

[39] Haiping Zhang, Hongfei Lin, Weizhi Wang, Ying Zheng, Peijun Hu. Hydroprocessing of waste cooking oil over a dispersed nano catalyst: Kinetics study and temperature effect. App. Cat. B 150-151 (2014), pp. 238-248.

[40] Octave Levenspiel. Chemical Reaction Engineering, Ind. Eng. Chem. Res. 38 (1999), pp. 4140.

[41] Charles N. Satterfield. Trickle-bed reactors. AlChe Journal 21 (1975), pp. 209-228.

[42] Lukasz Jeczmionek, Krystyna Porzycka-Semczuk. Hydrodeoxygenation, decarboxylation and decarbonylation reactions while co-processing vegetable oils over a NiMo hydrotreatment catalyst. Part I: Thermal effects - Theoretical considerations. Fuel 131 (2014), pp. 1-5.

[43] Vivek V. Ranade, Raghunath V. Chaudhari and Prashant R. Gunjal. Trickle Bed Reactors. Reactor Engineering & Applications (2011). ISBN: 978-0-444-52738-7

[44] F. Larachi, A. Laurent, N. Midoux, G. Wild. Experimental Study of a Trickle-bed Reactor Operating at High Pressure: Two Phase Pressure Drop and Liquid Saturation. Chem. Eng. Science 46 (1991), pp. 1233-1246.

[45] Gianetto, A., and V. Specchia, Trickle-bed Reactors: State of Art and Perspectives, Chem. Eng. Sci. 47 (1992), pp. 3197.

[46] Hans Korsten, Ulrich Hoffmann. Three Phase Reactor Model for Hydrotreating in Pilot Trickle-bed Reactors. AlChE Journal 42 (1996), pp. 1350-1360.

[47] Shigeo Goto, J.M. Smith. Trickle-Bed Reactor Perfomance. AlChE Journal 21 (1975), pp. 706-713.

[48] A.A. Forghani, M. Jafarian, P. Pendleton, D.M. Lewis. Mathematical modeling of a hydrocracking reactor for triglyceride conversion to biofuel: model establishment and validation. Int. J. Energy Res. 38 (2014), pp. 1624-1634.

[49] M.Alifanti, C.M.Visinescu. V.I.Parvulescu, P.Grange, G.Poncelet. Preparation and characterization of WOx-CeO2 catalysts. Studies in Surface Science and Catalysis 143 (2000), pp. 337-344.

[50] T. Kasza, J. Hancsok. Investigation of Fuel Components Produced by the Isomerization of Bio-paraffin Mixtures. Hungarian Journal of Industrial Chemistry 39 (2011), pp. 121-126.

[51] V. Calemma, S. Peratello and C. Perego. Hydroisomerization and hydrocracking of Long-Chain n-Alkanes on Pt/amorphous SiO2-Al2O3 catalyst. Reactivity and Reaction Pathway for Base Oil Formation. Ind. Eng. Chem. Res. 43 (2004), pp. 934-940.

[52] Oil Price Outlook. Web article from https://www.globalpetrolprices.com retrieved on the 26th of December of 2018.

[53] World Energy Council. World Energy Issues Monitor 2018. Assessing the energy agenda for Euope, pp. 48-81.

[54] International Maritime Organization (IMO). Guidance on the Development of a Ship Implementation Plan for the Consistent Implementation of the 0,5% sulfur limit under Marpol Annex VI, November 2018.

[55] Precios de los derivados del petróleo en Espana, information retrieved at www.datosmacro.com in December 2018.

[56] Chris Castanien. Renewable Diesel: Sustainable Hydrocarbon Fuel. Detroit Advisory Forum 17 April 2018.

[57] Neste Oil (2018). Palm and rapeseed oil prices. Data source: Thomson Reuters. Information retrieved from www.neste.com in December 2018.

[58] International Monetary Fund. Market Prices for Non-fuel and fuel commodities from 2014 to 2017. Information retrieved from www.imf.org in December 2018.

[59] Michael J.Girgis, and Y. Peter Tsao. Impact of Catalyst Metal-Acid Balance in n-Hexadecane Hydroisomerization and Hydrocracking. Ind. Eng. Chem. Res. 35 (1996), pp. 386-396.

[60] Nataliya Belinskaya, Emiliya Ivanchina, Elena Ivashkina, Evgeniya Frantsina,Galina Silko. Optimal technological parameters of diesel fuel hydroisomerization unit work investigation by means of mathematical modeling method. Procedia Chemistry 10 (2014), pp. 258-266.

[61] Towler, G.P. and Sinnott, R.K. Chemical engineering design: Principles, practice and economics of plant and process design. Butterworth-Heinemann, 2nd Edition (2012).

[62] R. Turton, R. C. Bailie, W. B. Whiting, and J. A. Shaeiwitz Analysis, synthesis and design of chemical processes. Prentice Hall, 3rd Edition (2008).

[63] Donald R. Woods. Rules of Thumb in Engineering Practice. Wiley-VCH, 1st edition (2007).

[64] Chemicals Technology. Neste Oil Biodiesel Plant. Information retrieved from https://www.chemicals-technology.com/projects/neste-oil-plant/ in December 2018.

[65] Eurostat Statistics. Electricity Price statistics. Information retrieved from https://ec.europa.eu/eurostat/statistics-explained/index.php/Electricity_price_statistics in December 2018.

[66] Charles R. Perry, Basic Design and Cost Data for MEA Treating Units. Portable Treaters Inc., Odessa, Texas.

[67] M.A. Ramos Carpio. Refino de petróleo, gas natural y petroquímica. Madrid, 1997.

[68] Tim J. Hilbers, Lisette M. J. Sprakel, Leon B. J. van den Enk, Bart Zaalberg, Henk van den Berg, Louis G. J. van der Ham. Green Diesel from Hydrotreated Vegetable Oil Process Design Study. Chem. Eng. Technol 38 (2015), pp. 1-8.

[69] Neste Oil. How to calculate Renewable Products margin. Information retrieved from https://www.neste.com in December 2018.